OXFORD JLB JOURNAL OF LEUKOCYTE BIOLOGY

*Journal of Leukocyte Biology*, 2025, **117**, qiaf107

**https://doi.org/10.1093/jleuko/qiaf107**
Advance access publication 22 July 2025
**Research Article**

# An IL-15-modified NKp30×HER2 trispecific NK cell engager enhances NK cell activation and tumor cell killing

Yaping Cheng,[1] Quanxiao Li,[1] Yu Kong,[1] Ailing Huang,[1] Zhenlin Yang,[2,*] Tianlei Ying,[1,2,*] and Yanling Wu[1,2,*]

[1]Key Laboratory of Medical Molecular Virology (MOE/NHC/CAMS) and Shanghai Institute of Infectious Disease and Biosecurity, School of Basic Medical Sciences, Fudan University, 130 Dong'an Road, Shanghai 200032, China
[2]Shanghai Engineering Research Center for Synthetic Immunology and Shanghai Key Laboratory of Lung Inflammation and Injury, Fudan University, 130 Dong'an Road, Shanghai 200032, China
*Corresponding authors: Zhenlin Yang, Shanghai Engineering Research Center for Synthetic Immunology and Shanghai Key Laboratory of Lung Inflammation and Injury, Fudan University, 130 Dong'an Road, Shanghai 200032, China. Email: yang_zhenlin@fudan.edu.cn; Tianlei Ying, Shanghai Engineering Research Center for Synthetic Immunology and Shanghai Key Laboratory of Lung Inflammation and Injury, Fudan University, 130 Dong'an Road, Shanghai 200032, China. tlying@fudan.edu.cn; Yanling Wu, Shanghai Engineering Research Center for Synthetic Immunology and Shanghai Key Laboratory of Lung Inflammation and Injury, Fudan University, 130 Dong'an Road, Shanghai 200032, China. yanlingwu@fudan.edu.cn.

## Abstract

Natural killer (NK) cells represent a promising effector population for tumor immunotherapy. Conventional NK cell engagers (NKCEs), primarily targeting CD16a, show efficacy but face limitations due to receptor polymorphisms and off-target toxicity. Here, we report the development and characterization of a novel trispecific NK cell engager (TriKE) simultaneously targeting the activating receptor NKp30 and the tumor-associated antigen HER2, integrated with a modified interleukin-15 (IL-15 N72D) fused to the IL-15Rα sushi domain (IL-15RαSu) to enhance NK cell proliferation and persistence. Protein expression and affinity analyses confirmed the proper formation of the fusion protein with high-affinity binding to NKp30, HER2, and IL-15 receptor components. Flow cytometry demonstrated dose-dependent binding of the TriKE to primary human NK cells and HER2$^+$ tumor cells. Functionally, the TriKE induced significantly greater NK cell activation, as measured by CD69 expression, compared with a bispecific engager lacking IL-15. Importantly, cytotoxicity assays revealed superior NK-mediated killing of HER2$^+$ tumor cells upon prolonged exposure, highlighting the immunostimulatory effect of the IL-15 moiety. These results establish the αNKp30 TriKE as a potent platform to redirect NK cytotoxicity against HER2$^+$ tumors, combining targeted receptor engagement with cytokine-driven activation to enhance NK cell–based cancer immunotherapy.

**Keywords:** IL-15, NK cell, NKp30, TriKE, tumor immunotherapy

## 1. Introduction

Natural killer cells are innate lymphoid effectors that play a crucial role in immune surveillance through direct cytotoxic activity against tumor and virally infected cells.[1,2] Their function is tightly regulated by a complex interplay of activating and inhibitory surface receptors.[3] Among recent immunotherapeutic developments, NKCEs represent a promising class of biologics designed to redirect NK cell cytotoxicity toward tumor targets in an antigen-specific manner.[4,5] These antibody-based constructs, commonly designed as bispecific or trispecific killer cell engagers (BiKEs or TriKEs), simultaneously engage NK cells and tumor cells. By bridging these two cell types, they facilitate the formation of an artificial immune synapse, thereby promoting efficient immune activation and targeted tumor cell lysis.[5]

Most NKCEs platforms rely on CD16a (FcγRIIIa), the classical Fc receptor on NK cells, to initiate antibody-dependent cellular cytotoxicity (ADCC).[6,7] Therapeutics such as AFM13, a tetravalent bispecific antibody composed of single-chain variable fragments (scFvs) targeting CD16a and CD30, have demonstrated potent antitumor activity against CD30$^+$ malignancies.[8] Similarly, E5C1, a BiKE assembled from single-domain antibodies targeting CD16a and HER2, effectively eliminates HER2$^+$ ovarian tumors in NK cell-humanized mouse models.[9,10] However, the clinical utility of CD16a-targeting engagers is limited by several intrinsic factors. Genetic polymorphisms in CD16a, such as the 158 V/F variant, result in variable anti-CD16a-binding affinities across individuals.[11,12] In addition, CD16a is susceptible to ADAM17-mediated proteolytic shedding upon NK cell activation, leading to decreased surface expression and reduced therapeutic efficacy.[3,13,14]

These challenges highlight the need for alternative NK cell activation strategies. NKp30, a member of the natural cytotoxicity receptor (NCR) family encoded by *NCR3*, has emerged as a compelling candidate.[2,15] NKp30 transduces activation signals upon engagement with its ligand B7-H6 through immunoreceptor tyrosine-based activation motifs (ITAMs),[16,17] independent of Fc-mediated pathways. Clinically, elevated *NCR3* expression correlates with improved prognosis in several tumor types, supporting a role for NKp30 in anti-tumor immune surveillance.[18]

To enhance the persistence and effector function of NK cells, interleukin-15 (IL-15), a common γ-chain cytokine that is essential for NK cell proliferation, survival, and activation, has been incorporated into TriKE constructs.[19] Notably, TriKE such as 1615133 (targeting CD16a and CD133) and 161519 (targeting CD16a and CD19) have demonstrated superior NK cell activation and cytotoxicity compared with their BiKEs counterparts that lacks the IL-15 component.[20,21]

Based on these insights, we developed a novel trispecific NK cell engager that targeting NKp30 and HER2, incorporating a modified

**Received:** June 5, 2025. **Revised:** June 20, 2025. **Accepted:** July 22, 2025. **Corrected and Typeset:** August 25, 2025

IL-15 (N72D mutant) fused to the IL-15Rα sushi domain via a flexible linker—drawing design inspiration from the ALT-803 cytokine complex.[22] HER2 was selected as the tumor antigen target due to its well-established role as a clinically validated and widely expressed tumor-associated antigen in various malignancies. This construct, termed αNKp30 TriKE, is engineered to: (i) direct NK cells to HER2$^+$ tumor cells via dual-target recognition and (ii) enhance NK cell expansion and persistence through IL-15 signaling.

In this study, we characterize the αNKp30 TriKE and compare its functional properties to a corresponding αNKp30 BiKE lacking the IL-15 module. We demonstrate that αNKp30 TriKE confers superior NK cell activation and cytotoxicity against HER2$^+$ tumor cells, particularly under extended stimulation conditions. Notably, our results highlight that NK cell engagers not reliant on CD16a can also achieve potent antitumor activity, offering an alternative strategy to overcome limitations associated with CD16a-based approaches. Collectively, our findings establish αNKp30 TriKE as a promising candidate for NK cell-based tumor immunotherapy.

## 2. Methods

### 2.1 Ethical statement

Peripheral blood mononuclear cells (PBMCs) were purchased from Milecell Biological Science & Technology Co., Ltd. The supplier confirmed that all human sample collection procedures were conducted in accordance with institutional ethical guidelines (Approval No. Z-ZJMS-21-08-001). Since the study used commercially available, de-identified human cells, no additional ethical approval was required from the authors' institutional review board.

### 2.2 Cell lines

The human non-small cell lung cancer cell line HCC827, human gastric cancer cell line NUGC-4, human breast cancer cell lines JIMT-1 and SKBR3, and human ovarian cancer cell line SKOV3 were obtained from Nanjing Cobioer Biosciences Co., Ltd. HCC827 cells were cultured in RPMI-1640 medium (Meilun) supplemented with 10% fetal bovine serum (FBS; Yeasen), 100 U/mL penicillin (Gibco), and 100 μg/mL streptomycin (Gibco). NUGC-4, JIMT-1, and SKOV3 cells were maintained in DMEM medium (Meilun) with the same supplements. SKBR3 cells were cultured in McCoy's 5A medium (Meilun) supplemented with 10% FBS (Yeasen), 100 U/mL penicillin (Gibco), and 100 μg/mL streptomycin (Gibco). All cells were incubated at 37°C in a humidified atmosphere containing 5% $CO_2$.

### 2.3 Plasmids construction

αNKp30 scFv or αHER2 scFv: the coding sequences for the VH and VL regions of scFvs were cloned into the bacterial expression vector pComb, linked by a flexible linker consisting of 3 repeats of the $G_4S$ sequence (3×$G_4S$). A signal peptide (MKKTAIAIAVALAGFATVAQAA) was added to the N-terminus to direct protein secretion, and both a 6×His tag and a FLAG tag were incorporated at the C-terminus to facilitate protein detection and purification. The αHER2 scFv sequence was obtained from reference,[23] and the αNKp30 scFv sequence was derived from Patent WO 2021/143858 A1.

αNKp30 BiKE: the coding sequences of αHER2 scFv and αNKp30 scFv were cloned into the eukaryotic expression vector pcDNA3.1, connected 3×G4S. A signal peptide (MFVFLVLLPLVSSQC) was added to the N-terminus, and both a 6×His tag and a FLAG tag were incorporated at the C-terminus.

αNKp30 TriKE: the coding sequences for αHER2 scFv, IL-15 (N72D)/IL-15RαSu, and αNKp30 scFv were cloned sequentially into pcDNA3.1 from N-terminus to C-terminus. The αHER2 scFv was linked to IL-15 (N72D) via a flexible SGGGGSGGGG linker. IL-15 (N72D) was fused to IL-15RαSu through the extended linker GGGSGGGGSGGGSGGGGSLQ, and IL-15RαSu was joined to αNKp30 scFv using the linker GGGSGGGSSGGGS. A signal peptide (MEWSWVFLFFLSVTTGVHS) was placed at the N-terminus, and both 6×His and FLAG tags were included at the C-terminus.

Antigens: The coding sequence of the extracellular domain of human NKp30, based on the sequence provided by Sino Biological, was cloned into the pSecTag expression vector. To enhance protein stability and facilitate purification and detection, an IgG1 Fc fragment was fused to the C-terminus of the NKp30 construct. The extracellular domain of HER2 was cloned and fused to the Fc fragment using the same strategy.

### 2.4 Protein expression and purification

The αNKp30 BiKE and αNKp30 TriKE proteins were expressed using the 293F eukaryotic expression system. After transient transfection and incubation, the culture supernatant was collected by centrifugation at 3,900 rpm for 15 min, then filtered through a 0.8 μm membrane. The clarified supernatant was incubated with Ni-smart beads (Smart-Lifesciences, SA035100) at 4°C overnight with gentle agitation to promote binding. The beads were washed with 25 mM imidazole in binding buffer to remove non-specifically bound proteins, and the target proteins were eluted using 250 mM imidazole. The eluate was then concentrated and buffer-exchanged into PBS using a 3 kDa molecular weight cut-off ultrafiltration unit (Millipore). Protein concentration was determined using a NanoDrop 2000 spectrophotometer (Thermo Fisher).

NKp30 and HER2 were expressed in the 293F system and purified using Protein G affinity chromatography. Culture supernatants were filtered through a 0.8 μm membrane and incubated overnight at 4°C with Protein G resin (GE Healthcare) under gentle agitation. The resin was collected, washed with PBS, and bound proteins were eluted with 0.1 M glycine buffer (pH 2.8). Eluates were immediately neutralized with 1 M Tris-HCl (pH 8.5) at a 20:1 (v/v) ratio, then concentrated using a 10 kDa molecular weight cut-off ultrafiltration device, and buffer-exchanged into PBS.

The scFvs were expressed in *Escherichia coli* HB2151 cultured in SB medium supplemented with 0.1 mg/mL ampicillin. When the $OD_{600}$ reached 0.6 to 0.8, protein expression was induced with 1 mM IPTG, and cells were incubated at 30°C for 14 h. Bacterial pellets were resuspended in PBS containing 0.5 M NaCl, treated with lysozyme, and incubated at 30 °C to promote lysis. After centrifugation, the supernatant was collected and filtered through a 0.8 μm membrane. Proteins were purified using Ni-NTA resin (GE Healthcare) as described above.

### 2.5 Enzyme-linked immunosorbent assay

The 96 half-well plates (Costar, Corning no. 3690) were coated with 200 ng per well of recombinant NKp30 or HER2 protein in PBS and incubated overnight at 4°C. After coating, the wells were washed with PBST (PBS with 0.05% Tween 20) and blocked with 5% bovine serum albumin (BSA) in PBS for 1 h at 37°C. Serial 3-fold dilutions of the test proteins were prepared in PBS and added to the wells, followed by incubation at 37°C for 90 min. Wells were then washed with PBST and incubated with anti-FLAG-HRP antibody (Sigma-Aldrich) for 45 min at 37°C. Peroxidase activity was visualized by adding ABTS substrate

(Invitrogen), and absorbance was measured at 405 nm using a microplate reader (BioTek).

## 2.6 Biolayer interferometry

The binding kinetics of αNKp30 TriKE to IL-15Rβ was measured using the OctetRED96 system (ForteBio). Amine Reactive 2nd Generation (AR2G) biosensors (Sartorius) were activated with 20 mM EDC (1-ethyl-3-[3-dimethylaminopropyl] carbodiimide hydrochloride) and 10 mM sulfo-NHS (N-hydroxysulfosuccinimide) according to the manufacturer's protocol. Activated sensors were loaded with 15 μg/mL recombinant IL-15Rβ (Sino Biological) and subsequently quenched with 1 M ethanolamine (pH 8.5). After establishing a baseline in PBST (PBS with 0.2% Tween-20), the sensors were immersed in a series of threefold serial dilutions of αNKp30 TriKE protein (starting at 1000 nM) for 300 s (association phase), followed by immersion in PBST for another 300 s (dissociation phase) at 37°C. Binding data were fitted using a 1:1 binding model in the ForteBio Data Analysis software (version 10.0). Dissociation constant ($K_D$) values were calculated from global fitting, and only curves with an $R^2 > 0.95$ were considered for kinetic interpretation.

## 2.7 Flow cytometry analysis of αNKp30 TriKE binding to cells

PBMCs were stained with fluorochrome-conjugated anti-CD3-FITC and anti-CD56-PerCP/Cy5.5 antibodies (BioLegend) in FPBS (PBS supplemented with 0.2% FBS). PBMCs or tumor cells were resuspended in FPBS and adjusted to a final concentration of $2.0 \times 10^7$ cells/mL. A total of 50 μL of the cell suspension was mixed with 50 μL of AF647-conjugated αNKp30 TriKE, previously diluted to the desired concentration in FPBS. The mixture was incubated on ice for 1 h in the dark. After incubation, the cells were washed twice with cold FPBS to remove unbound protein and resuspended in 200 μL FPBS. Cell surface fluorescence was analyzed using a BD LSRFortessa flow cytometer, and data were processed using FlowJo software (version 10).

## 2.8 NK cell activation assay

PBMCs were resuspended in RPMI-1640 complete medium at a final concentration of $5.0 \times 10^6$ cells/mL, and 100 μL was added to each well of a 96-well plate. αNKp30 TriKE, αNKp30 BiKE, and IL-15 were diluted to the indicated concentrations in culture medium, filtered through a 0.22 μm sterile filter, and 50 μL of each was added to the respective wells. Tumor cells were resuspended at $2.0 \times 10^6$ cells/mL in culture medium, and 50 μL was added to each well to achieve an effector-to-target (E:T) ratio of 5:1. Plates were gently mixed and incubated at 37°C for 4 h. Following incubation, cells were stained with Zombie Violet™ Fixable Viability Dye (Biolegend), and subsequently with anti-CD3-FITC, anti-CD56-APC, and anti-CD69-PE antibodies (Biolegend). Samples were acquired on a BD LSRFortessa flow cytometer, and data were analyzed using FlowJo software (version 10).

## 2.9 Cytotoxicity assay

PBMCs were resuspended in complete medium at a concentration of $1.0 \times 10^7$ cells/mL and serially diluted twofold to the desired effector cell densities. A volume of 100 μL of each dilution was added to the wells of a 96-well plate. αNKp30 TriKE or αNKp30 BiKE proteins were diluted to the indicated concentrations in culture medium, filtered through a 0.22 μm sterile filter, and 50 μL was added to the corresponding wells. Tumor cells were labeled with CFSE (Biolegend) according to the manufacturer's instructions, then resuspended in medium at a final concentration of $4 \times 10^5$ cells/mL. A volume of 50 μL of the labeled tumor cell suspension was added to each well. The mixtures were gently mixed and incubated at 37°C in a humidified incubator for either 4 or 20 h, as indicated. Following incubation, samples were transferred to flow cytometry tubes and stained with 2 μL of 7-AAD (BD Biosciences) to assess cell viability. Data acquisition was performed on a BD LSRFortessa flow cytometer, and analysis was conducted using FlowJo software (version 10).

## 2.10 Survical analysis

Survival analysis was conducted using the GEPIA2 web server (http://gepia2.cancer-pku.cn). Gene expression data for *NCR3* were obtained from the TCGA database. Overall survival (OS) was selected as the clinical endpoint, and patients were stratified into high- and low-expression groups based on the median expression level of *NCR3*. Survival curves were plotted with time in months, and statistical significance was determined using the log-rank test.

## 2.11 Statistical analysis

Data are presented as mean ± SD. Statistical analyses were performed using GraphPad Prism software (version 8.0). Comparisons between 2 groups were made using a 2-tailed unpaired *t*-test, while multiple group comparisons were assessed using 2-way ANOVA with Tukey's multiple comparisons test. $P < 0.05$ was considered statistically significant, with different levels denoted as $^*P < 0.05$, $^{**}P < 0.01$, $^{***}P < 0.001$, and $^{****}P < 0.0001$, respectively.

# 3. Results

## 3.1 NKp30 expression correlates with patient prognosis

To investigate the clinical relevance of NKp30 in anti-tumor immunity, we performed Kaplan-Meier survival analyses using TCGA datasets across various cancer types. Patients were stratified into high and low *NCR3* expression groups based on median expression levels. As shown in Fig. 1, elevated *NCR3* expression was significantly associated with improved overall survival in patients with skin cutaneous melanoma (SKCM; log-rank $P = 0.00051$; HR = 0.63), mesothelioma (MESO; $P = 0.039$; HR = 0.61), and head and neck squamous cell carcinoma (HNSC; $P = 0.0067$; HR = 0.69). These results support a potential protective role for NKp30 in these malignancies. The observed correlation between high *NCR3* expression and better prognosis suggests a role for NKp30 in enhancing anti-tumor immune surveillance, prompting further exploration of NKp30 as a therapeutic target for immune-based interventions.

## 3.2 Construction and characterization of αHER2×IL-15×αNKp30 TriKE

To potentiate NK cell-mediated cytotoxicity through NKp30 engagement and IL-15-driven activation, we developed a αNKp30 TriKE construct targeting HER2 and NKp30, incorporating IL-15 N72D fused to the IL-15RαSu. For comparison, a αNKp30 BiKE lacking the IL-15 module was also constructed (Fig. 2A). Both constructs consisted of scFvs against HER2 and NKp30, joined by flexible linkers to optimize spatial configuration.

The purity and molecular weights of the recombinant αNKp30 TriKE and αNKp30 BiKE proteins were confirmed by SDS-PAGE (Fig. 2B). To assess the biological functionality of the IL-15 module, we measured the binding affinity of αNKp30 TriKE to IL-15Rβ using Biolayer interferometry (BLI). The results demonstrated a dissociation constant of 33.90 ± 1.13 nM, confirming the effective

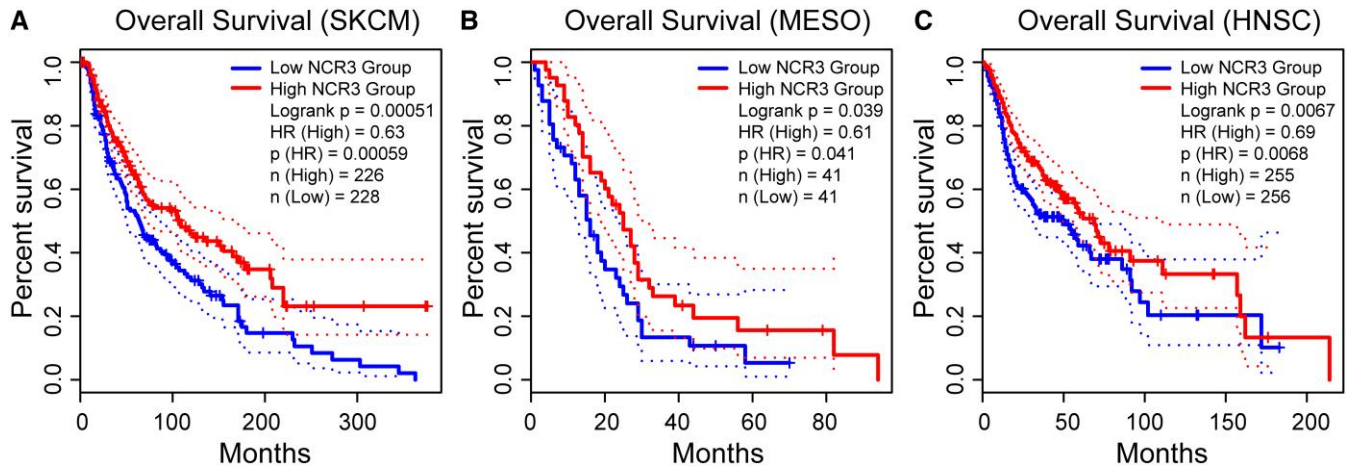


Fig. 1. Kaplan–Meier overall survival analyses stratified by *NCR3* expression levels in patients with different cancer types. Patients were divided into high and low *NCR3* expression groups based on median expression values. A) SKCM, B) MESO, and C) HNSC. Survival differences between groups were assessed using the log-rank test. Hazard ratios (HRs), *P* values, and sample sizes for each group are indicated in the plots.

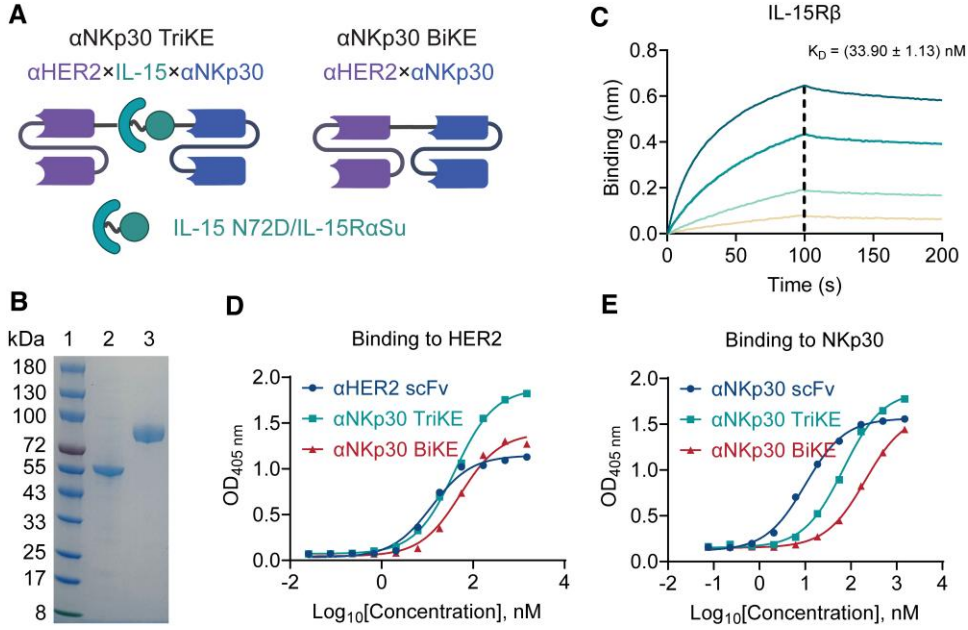


Fig. 2. Design and characterization of αNKp30 TriKE and αNKp30 BiKE constructs. A) Schematic representation of the αNKp30 TriKE and αNKp30 BiKE molecules. B) SDS-PAGE analysis confirming the molecular weights and purity of the αNKp30 TriKE and αNKp30 BiKE proteins. Lane 1: Protein marker; Lane 2: αNKp30 BiKE; Lane 3: αNKp30 TriKE. C) Binding kinetics of αNKp30 TriKE to human IL-15Rβ as determined by BLI. D and E) Binding of αNKp30 scFv, αNKp30 BiKE, and αNKp30 TriKE to HER2 (D) and NKp30 (E), measured by ELISA.

engagement of IL-15Rβ by αNKp30 TriKE (Fig. 2C). ELISA analyses further demonstrated that both engagers retained target-binding capability to HER2 and NKp30 (Fig. 2D, E), albeit with mildly reduced affinity compared with individual scFvs. Notably, αNKp30 TriKE displayed stronger NKp30 binding relative to αNKp30 BiKE (Table 1), suggesting that the incorporation of IL-15 may increase the spatial flexibility of the molecule, thereby enhancing its binding dynamics.

## 3.3 Binding profile of αNKp30 TriKE to NK cells and HER2-expressing tumor cell lines

To evaluate target cell binding, αNKp30 TriKE was conjugated with AF647 and assessed by flow cytometry. As shown in Fig. 3A, the labeled αNKp30 TriKE demonstrated robust binding to primary human NK cells at both 20 and 50 μg/mL concentrations, with over 95% of cells staining positive. Median fluorescence intensity (MFI) values plateaued across the 2 doses (Fig. 3B), suggesting saturable binding was achieved at 20 μg/mL.

To assess tumor binding, we first profiled HER2 expression levels across multiple tumor cell lines. Flow cytometric analysis revealed low HER2 expression in HCC827 and NUGC-4, intermediate in JIMT-1, and high expression in SKOV3 and SKBR3 (Fig. S1A). Binding assays with AF647-conjugated αNKp30 TriKE demonstrated effective, dose-dependent binding to $HER2^{high}$ SKOV3 and $HER2^{mid}$ JIMT-1 cells (Fig. 3C, D; Fig. S1B, C). Over 90% of cells were TriKE-positive at 20 μg/mL, accompanied by proportional increases in MFI values, indicative of efficient and concentration-dependent target engagement.

These results confirm that αNKp30 TriKE binds specifically and effectively to both primary NK cells and HER2-expressing tumor cells, with binding strength positively correlating with target antigen expression.

### 3.4 αNKp30 TriKE promotes superior NK cell activation compared to αNKp30 BiKE

To compare the stimulatory effects of αNKp30 BiKE and αNKp30 TriKE on NK cells, we co-cultured PBMCs with HER2$^+$ JIMT-1 tumor cells at an effector-to-target (E:T) ratio of 5:1. NK cell activation was assessed by measuring CD69 expression using flow cytometry. As shown in Fig. 4A, treatment with either αNKp30 BiKE or αNKp30 TriKE increased the CD69$^+$ NK cells relative to PBS and IL-15 controls. Notably, αNKp30 TriKE treatment induced significantly high CD69 expression (76.8%) compared to αNKp30 BiKE (61.4%), IL-15 (46.5%), or PBS (46.6%). Quantification of CD69$^+$ frequencies (Fig. 4B) confirmed a significant enhancement of NK cell activation by αNKp30 TriKE over αNKp30 BiKE ($P < 0.01$). These findings highlight the immune-potentiating effect conferred by IL-15 incorporation into the αNKp30 TriKE construct and support its superior ability to activate NK cells in the presence of HER2$^+$ tumor targets.

**Table 1.** $EC_{50}$ values (nM) for the binding of protein constructs to HER2 and NKp30.

| Protein | HER2 (nM) | NKp30 (nM) |
|---|---|---|
| αHER2 scFv | 12.46 | n.a. |
| αNKp30 scFv | n.a. | 10.09 |
| αNKp30 BiKE | 52.53 | 205.10 |
| αNKp30 TriKE | 38.81 | 67.89 |

Abbreviations: $EC_{50}$, half maximal effective concentration; n.a., not applicable.

### 3.5 αNKp30 TriKE enhances PBMC-mediated cytotoxicity against HER2$^+$ tumor cells

To assess the cytotoxic potential of αNKp30 BiKE and αNKp30 TriKE, HER2$^+$ tumor cell lines JIMT-1 and SKOV3 were labeled with CFSE and co-cultured with PBMCs at varying E:T ratios. Cytotoxicity was quantified by detecting the proportion of CFSE$^+$ 7-AAD$^+$ tumor cells via flow cytometry. After 4 h of incubation, minimal cytotoxicity was observed in the PBS group across all E:T ratios, and no significant increase in target cell death was noted with increasing effector numbers (Fig. S2). In contrast, both αNKp30 BiKE and αNKp30 TriKE significantly augmented PBMC-mediated cytotoxicity compared to PBS ($P < 0.0001$), confirming their role in facilitating NK cell-dependent tumor killing. However, under short-term conditions, αNKp30 TriKE and αNKp30 BiKE elicited comparable cytolytic effects in JIMT-1 cells, with no statistically significant differences between the two.

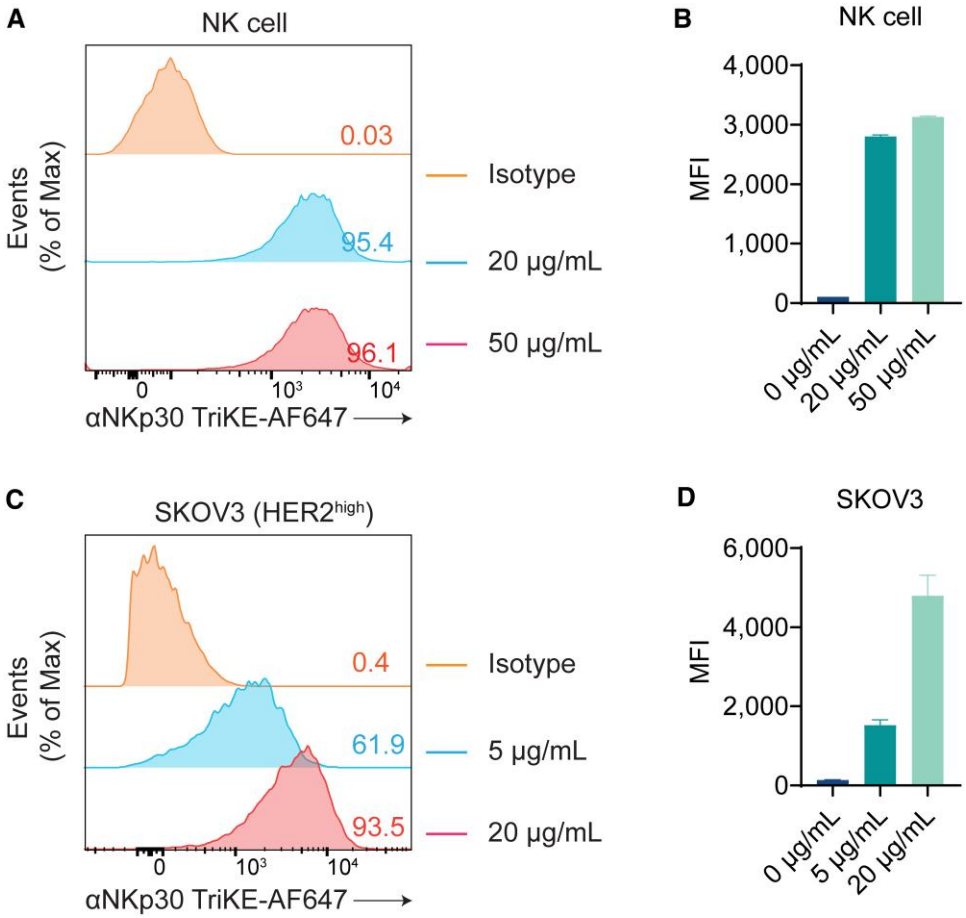


Fig. 3. Flow cytometric analysis of the cellular binding profile of αNKp30 TriKE-AF647 to NK cells and HER2$^+$ tumor cells. A) Representative histogram plots showing the percentage of αNKp30 TriKE-AF647 positive NK cells at indicated concentrations. B) Quantification of MFI corresponding to αNKp30 TriKE-AF647 binding to NK cells ($n = 3$). C) Representative histogram plots showing the percentage of αNKp30 TriKE-AF647 positive SKOV3 cells. D) MFI quantification of αNKp30 TriKE-AF647 binding to SKOV3 cells ($n = 3$). Data are presented as mean ± SD.

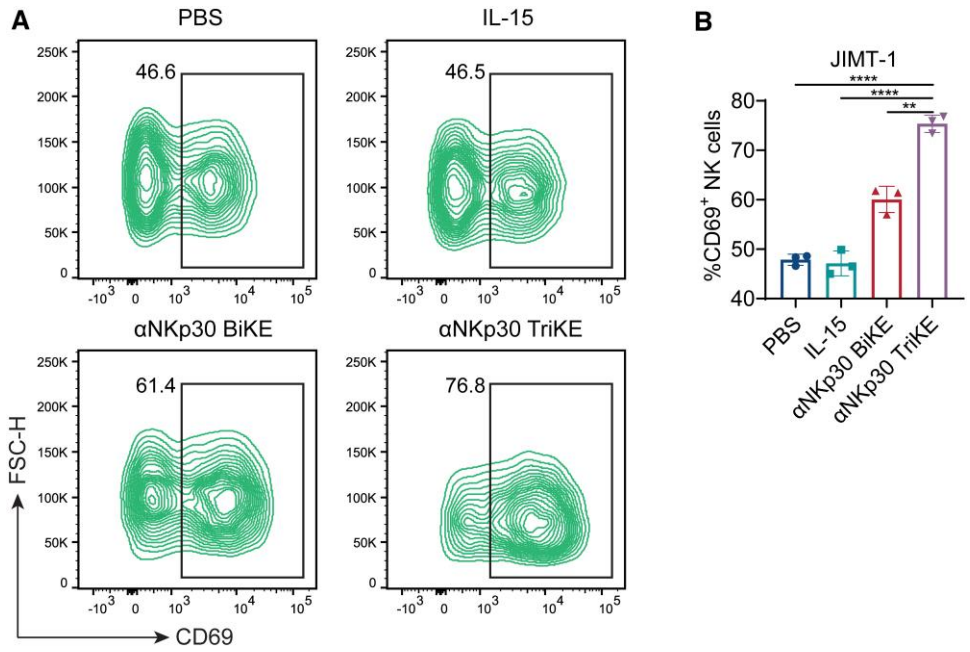


Fig. 4. Flow cytometric analysis of NK cell activation in response to αNKp30 TriKE in the presence of JIMT-1 tumor cells. A) Representative contour plots showing the percentage of CD69⁺ NK cells following co-culture with JIMT-1 cells and treatment with PBS, IL-15, αNKp30 BiKE, or αNKp30 TriKE. B) Quantification of CD69⁺ NK cells across different treatment conditions ($n = 3$). Data are presented as mean ± SD. Statistical significance was determined using 2-tailed unpaired $t$-test. $^{**}P < 0.01$; $^{****}P < 0.0001$.

To capture the delayed activation kinetics of IL-15, we extended the incubation period to 20 h. Under these conditions, PBMCs alone exhibited modest basal killing, but the presence of αNKp30 BiKE or αNKp30 TriKE further increased cytotoxicity in both JIMT-1 and SKOV3 cells (Fig. 5A–D). Furthermore, αNKp30 TriKE elicited significantly greater tumor cell killing than αNKp30 BiKE at all E:T ratios, consistent with enhanced and sustained NK cell activation. Taken together, these data demonstrate that while both engagers enhance NK cell-mediated cytotoxicity against HER2⁺ tumor cells, the inclusion of IL-15 in the αNKp30 TriKE design confers a superior and durable anti-tumor response, particularly under prolonged exposure conditions.

## 4. Discussion

NKCEs have gained increasing attention as a promising class of immunotherapeutics, particularly suited for treating tumors that exhibit resistance to conventional T cell-based strategies.[6,24] Among the most clinically advanced NKCEs are AFM13 and AFM24, which target CD30 and EGFR, respectively, and are currently undergoing evaluation in phase II clinical trials.[6] These developments underscore the translational potential of NKCEs in cancer immunotherapy. However, a majority of NKCEs developed to date rely on engagement of CD16a (FcγRIIIa) to mediate ADCC.[6,7,25] While effective, this mechanism presents several notable limitations. CD16a is not restricted to NK cells but is also expressed on multiple myeloid cell subsets,[26] posing a risk of off-target immune activation and associated toxicities, including cytokine release syndrome. Moreover, CD16a is prone to proteolytic shedding by ADAM17 upon NK cell activation, resulting in downregulation of surface receptor levels and attenuation of cytolytic function over time.[3,13,14] These challenges underscore a need for NKCEs that leverage alternative NK-specific activating receptors to improve both safety and therapeutic durability.

Recent efforts have focused on exploiting NK cell-restricted activating receptors such as NKG2D, NKp46, and NKp30.[27–29] Notably, many approaches have combined these with CD16a engagement to synergistically enhance NK cell activation. Initial NKp30-targeting NKCEs employed engineered ligands such as B7-H6 variants[30]; however, advancements in nanobody and yeast display technologies have enabled the generation of high-affinity single-domain antibodies (VHHs) with enhanced specificity and modular design. Contemporary NKp30-directed NKCEs often utilize IgG-like scaffolds incorporating Fc-silencing mutations (eg LALAPG) to mitigate FcγR binding.[31,32]

Building upon these advancements, we developed a trispecific NK cell engager, termed αNKp30 TriKE, which uniquely combines specificity for NKp30 and HER2 with an IL-15-based cytokine signaling module. Inspired by the design of ALT-803, our construct incorporates a modified IL-15 superagonist (N72D) fused to the IL-15Rα sushi domain, designed to enhance NK cell proliferation, survival, and sustained effector function. To our knowledge, this represents the first NKp30-targeting TriKE to incorporate such an IL-15 superagonist configuration. Functional analyses demonstrated that αNKp30 TriKE robustly activated NK cells and enhanced cytotoxicity compared with a corresponding αNKp30 BiKE lacking the IL-15 module, highlighting the pivotal role of cytokine-mediated stimulation in sustaining NK cell function.

Interestingly, kinetic profiling of cytotoxic activity revealed that the immunological benefits of IL-15 are time-dependent. In short-term (4 h) cytotoxicity assays, both αNKp30 TriKE and αNKp30 BiKE elicited comparable levels of tumor cell lysis, suggesting that IL-15 does not significantly augment immediate NK killing capacity. However, under prolonged stimulation (20 h), the αNKp30 TriKE induced markedly greater cytotoxicity, consistent with the well-established role of IL-15 in supporting NK cell persistence, expansion, and long-term functional activity.

Another noteworthy finding was the discordance between HER2 expression levels and cytolytic efficacy. Although SKOV3

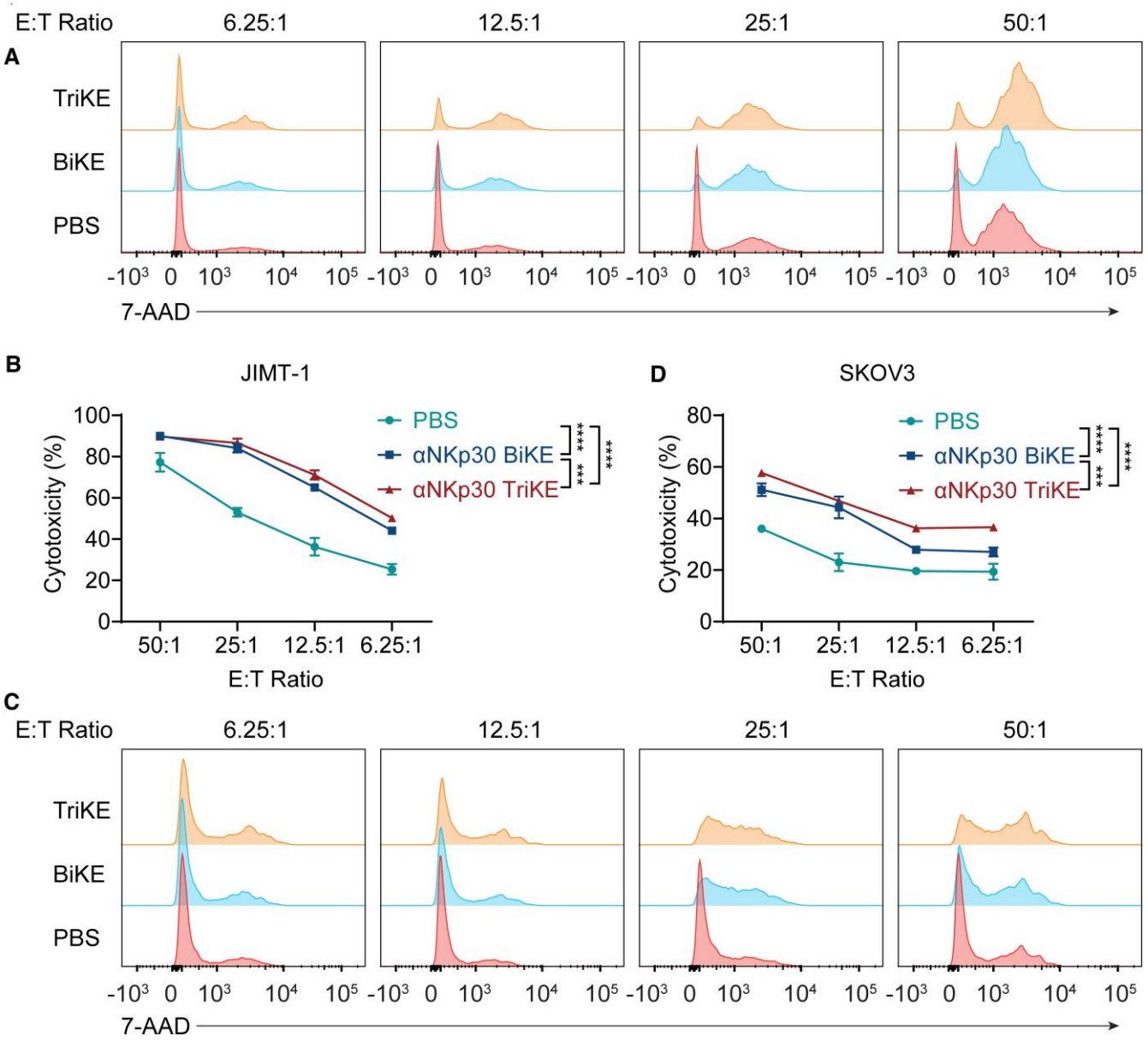


Fig. 5. Flow cytometric analysis of tumor cell killing mediated by PBMCs in the presence of αNKp30 TriKE or αNKp30 BiKE. A and C) Representative flow cytometry histograms showing tumor cell killing at varying E:T ratios, assessed by 7-AAD staining of CFSE-labeled target cells. JIMT-1 (A) and SKOV3 (C) cells were labeled with CFSE and co-cultured with PBMCs in the presence of αNKp30 TriKE or αNKp30 BiKE for 20 h. Tumor cell death was determined by the percentage of $CFSE^+$ $7\text{-}AAD^+$ cells. B and D) Quantification of cytotoxicity against JIMT-1 (B) and SKOV3 (D) cells across different E:T ratios ($n = 4$). Data are presented as mean ± SD. Statistical significance was determined by 2-way ANOVA with Tukey's multiple comparisons test. ***$P < 0.001$; ****$P < 0.0001$.

cells exhibited higher surface HER2 expression than JIMT-1 cells, αNKp30 TriKE induced more potent lysis of JIMT-1. This suggests that antigen density alone is not a reliable predictor of NKCE efficacy. Instead, intrinsic tumor factors such as sensitivity to NK cell–mediated lysis, expression of stress-induced ligands, and the presence of immune evasion mechanisms are likely to contribute to the observed differences in therapeutic response and warrant further investigation.[33–35]

In conclusion, our study introduces a novel IL-15 fused, NKp30-directed TriKE as a promising strategy for the treatment of tumor cells. By circumventing the limitations of CD16a-based targeting and integrating NK-specific receptor engagement with cytokine-driven activation, this platform offers a more selective and durable approach to NK cell-based immunotherapy.

## Author contributions

Y.C. and Y.W. conceived the study and designed the methodology. Y.C., Q.L., Y.K., and A.H. performed the experiments and analyzed the data. Y.C. wrote the original draft, and Y.W. and T.Y. reviewed and edited the manuscript. T.Y., Y.W., and Z.Y. supervised the project and acquired funding. All authors have read and agreed to the published version of the manuscript.

## Supplementary material

Supplementary material is available at *Journal of Leukocyte Biology* online.

## Funding

This work was supported by the National Natural Science Foundation of China (82394453, 92459301), Science and Technology Commission of Shanghai Municipality (23XD1400800), Fudan University (24FCB09, FudanX24AI043), Shanghai Municipal Health Commission (GWVI-11.2-YQ46), and the Shanghai Frontiers Science Center of Pathogenic Microorganisms and Infection.

*Conflicts of interest*. The authors declare no conflicts of interest.

## Data availability

All data needed to evaluate the conclusions in the paper are present in the paper.

## References

1. Vivier E, *et al.* Natural killer cell therapies. *Nature*. 2024:626:727–736. https://doi.org/10.1038/s41586-023-06945-1
2. Maskalenko NA, Zhigarev D, Campbell KS. Harnessing natural killer cells for cancer immunotherapy: dispatching the first responders. *Nat Rev Drug Discov*. 2022:21:559–577. https://doi.org/10.1038/s41573-022-00413-7
3. Myers JA, Miller JS. Exploring the NK cell platform for cancer immunotherapy. *Nat Rev Clin Oncol*. 2021:18:85–100. https://doi.org/10.1038/s41571-020-0426-7
4. Bottino C, Picant V, Vivier E, Castriconi R. Natural killer cells and engagers: powerful weapons against cancer. *Immunol Rev*. 2024:328:412–421. https://doi.org/10.1111/imr.13384
5. Zhang M, Lam KP, Xu S. Natural killer cell engagers (NKCEs): a new frontier in cancer immunotherapy. *Front Immunol*. 2023:14:1207276. https://doi.org/10.3389/fimmu.2023.1207276
6. Fenis A, Demaria O, Gauthier L, Vivier E, Narni-Mancinelli E. New immune cell engagers for cancer immunotherapy. *Nat Rev Immunol*. 2024:24:471–486. https://doi.org/10.1038/s41577-023-00982-7
7. Nikkhoi SK, Li G, Hatefi A. Natural killer cell engagers for cancer immunotherapy. *Front Oncol*. 2024:14:1483884. https://doi.org/10.3389/fonc.2024.1483884
8. Wu J, Fu J, Zhang M, Liu D. AFM13: a first-in-class tetravalent bispecific anti-CD30/CD16A antibody for NK cell-mediated immunotherapy. *J Hematol Oncol*. 2015:8:96. https://doi.org/10.1186/s13045-015-0188-3
9. Nikkhoi SK, *et al.* Bispecific killer cell engager with high affinity and specificity toward CD16a on NK cells for cancer immunotherapy. *Front Immunol*. 2022:13:1039969. https://doi.org/10.3389/fimmu.2022.1039969
10. Khoshtinat Nikkhoi S, *et al.* Bispecific immune cell engager enhances the anticancer activity of CD16+ NK cells and macrophages in vitro, and eliminates cancer metastasis in NK humanized NOG mice. *J Immunother Cancer*. 2024:12:e008295. https://doi.org/10.1136/jitc-2023-008295
11. Nimmerjahn F, Ravetch JV. Fcγ receptors as regulators of immune responses. *Nat Rev Immunol*. 2008:8:34–47. https://doi.org/10.1038/nri2206
12. Bruhns P, *et al.* Specificity and affinity of human Fcγ receptors and their polymorphic variants for human IgG subclasses. *Blood*. 2009:113:3716–3725. https://doi.org/10.1182/blood-2008-09-179754
13. Romee R, *et al.* NK cell CD16 surface expression and function is regulated by a disintegrin and metalloprotease-17 (ADAM17). *Blood*. 2013:121:3599–3608. https://doi.org/10.1182/blood-2012-04-425397
14. Jing Y, *et al.* Identification of an ADAM17 cleavage region in human CD16 (FcγRIII) and the engineering of a non-cleavable version of the receptor in NK cells. *PLoS One*. 2015:10:e0121788. https://doi.org/10.1371/journal.pone.0121788
15. Huntington ND, Cursons J, Rautela J. The cancer-natural killer cell immunity cycle. *Nat Rev Cancer*. 2020:20:437–454. https://doi.org/10.1038/s41568-020-0272-z
16. Matta J, *et al.* Induction of B7-H6, a ligand for the natural killer cell-activating receptor NKp30, in inflammatory conditions. *Blood*. 2013:122:394–404. https://doi.org/10.1182/blood-2013-01-481705
17. Fiegler N, *et al.* Downregulation of the activating NKp30 ligand B7-H6 by HDAC inhibitors impairs tumor cell recognition by NK cells. *Blood*. 2013:122:684–693. https://doi.org/10.1182/blood-2013-02-482513
18. Semeraro M, *et al.* Clinical impact of the NKp30/B7-H6 axis in high-risk neuroblastoma patients. *Sci Transl Med*. 2015:7:283ra255. https://doi.org/10.1126/scitranslmed.aaa2327
19. Ma S, Caligiuri MA, Yu J. Harnessing IL-15 signaling to potentiate NK cell-mediated cancer immunotherapy. *Trends Immunol*. 2022:43:833–847. https://doi.org/10.1016/j.it.2022.08.004
20. Schmohl JU, *et al.* Engineering of anti-CD133 trispecific molecule capable of inducing NK expansion and driving antibody-dependent cell-mediated cytotoxicity. *Cancer Res Treat*. 2017:49:1140–1152. https://doi.org/10.4143/crt.2016.491
21. Felices M, *et al.* Novel CD19-targeted TriKE restores NK cell function and proliferative capacity in CLL. *Blood Adv*. 2019:3:897–907. https://doi.org/10.1182/bloodadvances.2018029371
22. Xu W, *et al.* Efficacy and mechanism-of-action of a novel superagonist interleukin-15: interleukin-15 receptor αSu/Fc fusion complex in syngeneic murine models of multiple myeloma. *Cancer Res*. 2013:73:3075–3086. https://doi.org/10.1158/0008-5472.CAN-12-2357
23. Ahmadzadeh M, Farshdari F, Nematollahi L, Behdani M, Mohit E. Anti-HER2 scFv expression in *Escherichia coli* SHuffle T7 express cells: effects on solubility and biological activity. *Mol Biotechnol*. 2020:62:18–30. https://doi.org/10.1007/s12033-019-00221-2
24. Lin H, *et al.* Characterization and comparative analysis of multifunctional natural killer cell engagers during antitumor responses. *Cell Rep Med*. 2025:6:102117. https://doi.org/10.1016/j.xcrm.2025.102117
25. Shin MH, Oh E, Minn D. Current developments in NK cell engagers for cancer immunotherapy: focus on CD16A and NKp46. *Immune Netw*. 2024:24:e34. https://doi.org/10.4110/in.2024.24.e34
26. Galvez-Cancino F, *et al.* Fcγ receptors and immunomodulatory antibodies in cancer. *Nat Rev Cancer*. 2024:24:51–71. https://doi.org/10.1038/s41568-023-00637-8
27. von Strandmann EP, *et al.* A novel bispecific protein (ULBP2-BB4) targeting the NKG2D receptor on natural killer (NK) cells and CD138 activates NK cells and has potent antitumor activity against human multiple myeloma in vitro and in vivo. *Blood*. 2006:107:1955–1962. https://doi.org/10.1182/blood-2005-05-2177
28. Demaria O, *et al.* Antitumor immunity induced by antibody-based natural killer cell engager therapeutics armed with not-alpha IL-2 variant. *Cell Rep Med*. 2022:3:100783. https://doi.org/10.1016/j.xcrm.2022.100783
29. Gauthier L, *et al.* Control of acute myeloid leukemia by a trifunctional NKp46-CD16a-NK cell engager targeting CD123. *Nat Biotechnol*. 2023:41:1296–1306. https://doi.org/10.1038/s41587-022-01626-2
30. Pekar L, *et al.* Affinity maturation of B7-H6 translates into enhanced NK cell-mediated tumor cell lysis and improved proinflammatory cytokine release of bispecific immunoligands via NKp30 engagement. *J Immunol*. 2021:206:225–236. https://doi.org/10.4049/jimmunol.2001004

31. Klausz K, *et al.* Multifunctional NK cell-engaging antibodies targeting EGFR and NKp30 elicit efficient tumor cell killing and proinflammatory cytokine release. *J Immunol*. 2022:209:1724–1735. https://doi.org/10.4049/jimmunol.2100970
32. Boje AS, *et al.* Impact of antibody architecture and paratope valency on effector functions of bispecific NKp30 x EGFR natural killer cell engagers. *MAbs*. 2024:16:2315640. https://doi.org/10.1080/19420862.2024.2315640
33. Paczulla AM, *et al.* Absence of NKG2D ligands defines leukaemia stem cells and mediates their immune evasion. *Nature*. 2019:572:254–259. https://doi.org/10.1038/s41586-019-1410-1
34. Oh SC, *et al.* Ngr1 is an NK cell inhibitory receptor that destabilizes the immunological synapse. *Nat Immunol*. 2023:24:463–473. https://doi.org/10.1038/s41590-022-01394-w
35. Li Y, *et al.* IGSF8 is an innate immune checkpoint and cancer immunotherapy target. *Cell*. 2024:187:2703–2716.e2723. https://doi.org/10.1016/j.cell.2024.03.039